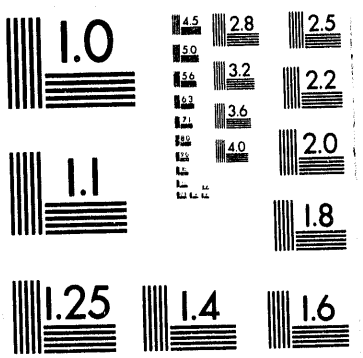
1.0
1.1
1.25
1.4
1.6
1.8
2.0
2.2
2.5
2.8
3.2
3.6
4.0
4.5
5.0
5.6
6.3
7.1
8.0
9.0

1 of 1

2

Factors governing selection of operating frequency for subsurface-imaging synthetic-aperture radar

Billy C. Brock, Ward E. Patitz

Sandia National Laboratories, Antenna Development Department
Albuquerque, New Mexico 87185-0531

ABSTRACT

A subsurface-imaging synthetic-aperture radar (SISAR) has potential for application in areas as diverse as non-proliferation programs for nuclear weapons to environmental monitoring. However, subsurface imaging is complicated by propagation loss in the soil and surface-clutter response. Both the loss and surface-clutter response depend on the operating frequency. This paper examines several factors which provide a basis for determining optimum frequencies and frequency ranges which will allow synthetic-aperture imaging of buried targets. No distinction can be made between objects at different heights when viewed with a conventional imaging radar (which uses a one-dimensional synthetic aperture), and the return from a buried object must compete with the return from the surface clutter. Thus, the signal-to-clutter ratio is an appropriate measure of performance for a SISAR. A parameter-based modeling approach is used to model the complex dielectric constant of the soil from measured data obtained from the literature. Theoretical random-surface scattering models, based on statistical solutions to Maxwell's equations, are used to model the clutter. These models are combined to estimate the signal-to-clutter ratio for canonical targets buried in several soil configurations. Results indicate that the HF spectrum (3-30 MHz), although it could be used to detect certain targets under some conditions, has limited practical value for use with SISAR, while the upper VHF through UHF spectrum (~100 MHz - 1 GHz) shows the most promise for a general purpose SISAR system. Recommendations are included for additional research.

1. INTRODUCTION

A subsurface-imaging synthetic-aperture radar (SISAR) offers a major advantage over a conventional ground-penetrating radar (GPR) because it resolves a scene into pixels which are much smaller than the antenna beamwidth. It achieves this resolution by focusing the beam with a large synthetic aperture. However, most conventional synthetic-aperture radars (SAR) operate at higher microwave frequencies which do not significantly penetrate below the soil surface. This study attempts to provide a basis for determining optimum frequencies which will allow synthetic-aperture imaging of buried targets. We begin with the assumption that the SISAR transmitter power and receiver noise figure can be chosen so that the radar sensitivity is limited by clutter (surface scattering) rather than thermal noise. Thus, the measure of performance to be examined is the ratio of the signal power received from a buried target to the power received from surface-clutter scattering, the signal-to-clutter ratio, S/C.

A conventional SAR uses a one-dimensional synthetic aperture, and produces a two-dimensional image. The synthetic aperture provides resolution in the along-track dimension, while the signal bandwidth provides resolution in the cross-track dimension. Depth and height are not available, except to the extent that target layover can be utilized to estimate height. The one-dimensional synthetic aperture does not provide a mechanism for distinguishing the returns from buried objects from those of the surface clutter or of objects on the surface. In fact, in order for a buried object to be detected by conventional SAR algorithms, its return must exceed that of the surface clutter in the same and adjacent pixels. It becomes obvious that maximizing the signal-to-clutter ratio is necessary for the success of a SISAR using a one-dimensional synthetic aperture. While unconventional SAR techniques are being proposed and studied[1], this work addresses the maximization of S/C necessary to allow the conventional techniques to be successful.

This study begins with a simple, back-of-the-envelope analysis in order to show the qualitative behavior of the signal-to-clutter ratio. This simple calculation is important because it provides the basis for understanding the frequency dependence of S/C. Following this are signal-to-clutter estimates based on more comprehensive and detailed models of soil properties, random-surface scattering, and canonical targets. From these estimates and the detailed analysis, we draw conclusions about the choice of operating frequencies, and recommendations for additional studies are given.

2. BACK-OF-THE-ENVELOPE ANALYSIS

Before examining the results of a more comprehensive and detailed analysis, it will be useful to characterize the signal-to-clutter ratio in a qualitative way to determine its approximate behavior as a function of frequency. This approach will demonstrate that an optimum frequency range exists for a SISAR, and will show how it depends on the parameters of the problem.

2.1 Target models

We begin a qualitative analysis by describing the behavior of targets of interest. Target behavior depends on its size with respect to the wavelength, its composition, its shape, the polarization of the of the transmitted and received signals, and the direction from which it is viewed. For this discussion, size and shape are of primary importance. For simplicity, conducting objects will be assumed. There will be three wavelength regions of interest: 1) the Rayleigh region where the object is small with respect to the wavelength, 2) the resonance region where the object is similar in size to a wavelength, and 3) the physical optics region where the object is large with respect to a wavelength. Calculation of the radar cross section of an object in the resonance region is a complex problem. However, for the qualitative analysis of this section, it is sufficient to model the target as a conducting object in either the Rayleigh or physical optics region. For objects in the physical optics region, curvature (shape) of the object's surface becomes important. The following model will be used

$$\sigma_{tgt} = \begin{cases} \sigma_0 \left(\dfrac{f}{f_a} \right)^4, & \text{Rayleigh object, } a < \lambda \\ \sigma_0 \left(\dfrac{f}{f_a} \right)^2, & \text{flat plate, corner reflector (physical optics, zero finite radii of curvature), } a > \lambda \\ \sigma_0 \left(\dfrac{f}{f_a} \right), & \text{cylinder (physical optics, single finite radius of curvature), } a > \lambda \\ \sigma_0, & \text{sphere, ellipsoid (physical optics, two finite radii of curvature), } a > \lambda \end{cases}, \tag{1}$$

where a is a characteristic dimension of the object, f_a is the frequency at which a is about one wavelength (λ) in the medium, and σ_0 is the radar cross section (square meters) when $f = f_a$.

2.2 Signal attenuation

The signal received from the target will be reduced by a transmission coefficient, $T = T_{ag} T_{ga}$, which accounts for the coupling from the air into the ground (T_{ag}) and from beneath the ground into the air (T_{ga}). This transmission coefficient will depend on the electric permittivity of the soil ($\varepsilon = \varepsilon_r \varepsilon_0$), which is frequency dependent, and on the magnetic permeability, $\mu = \mu_r \mu_0$. We will assume $\mu_r = 1$, although some soils have magnetic properties which must be included. The transmission coefficient represents a loss and $|T| < 1$.

In addition, the signal will be attenuated as it propagates through the soil. The two-way loss factor is

$$L = e^{-4\alpha f d}, \tag{2}$$

where

$$\alpha = -\mathrm{Im}\left\{ \frac{2\pi\sqrt{\varepsilon_r}}{c} \right\}, \tag{3}$$

d is the one-way distance the signal travels in the ground, and c is the speed of light in the vacuum.

2.3 Clutter model

The surface clutter from the ground is described by a scattering coefficient σ^0 which is a radar cross section per unit area of illuminated ground. σ^0 will depend on the roughness scale of the surface as well as on the dielectric constant and the angle of incidence. For this qualitative calculation, we will model σ^0 as

$$\sigma^0 = \varsigma\left(\frac{f}{f_\varsigma}\right)^m, \tag{4}$$

where ς is the value of σ^0 at $f = f_\varsigma$. Skolnik[2] presents data which suggest that $0 \le m \le 2$, but points out the frequency-variation data on which he bases that claim are crude.

In the SISAR image, the clutter return will be determined by the pixel area. We will assume that the synthetic-aperture radar has a resolution which is inversely proportional to the center frequency f. This is equivalent to assuming a constant percentage bandwidth for any center frequency, and represents constant complexity in the radar hardware and imaging algorithms. By assuming the azimuth and range resolutions are approximately the same, the area of a pixel on the surface is given by

$$A_p = \left(\frac{c}{2\delta f}\right)^2, \tag{5}$$

where δ is the fractional bandwidth of the radar. Thus the surface-clutter cross section is

$$C = \sigma^0 A_p = \varsigma\left(\frac{c}{2\delta}\right)^2 f^{m-2}. \tag{6}$$

2.4 Signal-to-clutter estimate

The signal-to-clutter ratio, S/C, can now be estimated by combining (1), (2), and (6)

$$S/C = \frac{\sigma_{tgt} L}{C} = \frac{T\sigma_0 f_\varsigma^m}{\varsigma\left(\frac{c}{2\delta}\right)^2 f_a^n} e^{-4\alpha f d} f^{n-m+2}. \tag{7}$$

2.5 Optimum frequency for maximum signal-to-clutter ratio

The maximum signal-to-clutter ratio occurs when

$$\frac{\partial S/C}{\partial f} = 0. \tag{8}$$

If we assume that ε_r is a slowly varying function of f, so that $\partial\alpha/\partial f$ and $\partial T/\partial f$ can be ignored, the optimum frequency is

$$f_{opt} \approx \frac{n-m+2}{4\alpha d}. \tag{9}$$

Although (9) is based on a simple back-of-the-envelope style calculation, it is very useful in estimating the appropriate frequency range for a SISAR application. It is gratifying to see that (9) predicts that the optimum frequency decreases as soil loss, α, and target depth, d, increase in agreement with what intuition tells us. However, it is interesting to see that for a particular target class, soil type, and burial depth, there is an *optimum* frequency which maximizes the signal-to-clutter ratio, and *decreasing* (or *increasing*) the frequency from this optimum will *degrade* the signal-to-clutter ratio. Further, the optimum frequency is higher for small targets (Rayleigh model, $n = 4$) than for any of the large targets (physical optics models, $n = 0,1$, or 2). The optimum frequency will be higher for flat targets ($n = 2$) than for cylinders ($n = 1$) or spheres ($n = 0$). If all other parameters remain constant, large spheres will have the lowest optimum frequency. Clearly the optimum frequency will be different for each different application.

2.6 Simple example

Suppose it is desired to find a small (Rayleigh) target located 5 m below the surface in soil resembling dry sand ($\varepsilon_r \approx 2.5 - 0.03i$). The optimum frequency predicted by (9) with $m = 2$ is about 1 GHz. Note that this is consistent with conclusions in the literature that the frequency of 1.3 GHz used on SIR-A is within the optimum range for depth penetration into sand[2]. The optimum frequency is reduced to about 100 MHz if the same object is buried 50 m below the surface. In a more lossy, wet soil with $\varepsilon_r = 5 - 5i$ with the same object buried 1 m below the surface, the optimum frequency is about 47 MHz.

This back-of-the-envelope analysis is approximate and better models are needed in order to more accurately predict the frequency dependence of the signal-to-clutter ratio. In particular, a good model (or models) is needed for the dielectric constant of soil since it is a dispersive (frequency dependent) media, and for the backscattering coefficient at the air-soil interface. The following results are based on detailed models for the soil dielectric constant, the surface clutter, and the target radar cross section.

3. MODELS USED IN THE COMPREHENSIVE ANALYSIS

The models used in the detailed analysis will be briefly described here. Additional details concerning these models are contained in a recent Sandia National Laboratories report[4].

3.1 Soil properties

Rather than simply applying a curve fit to measured data in order to obtain a model for the complex relative dielectric constant, ε_r, a model based on the physics of materials is used. The material is assumed to behave as a collection of electric dipoles, and the dielectric constant describes the interaction of the electromagnetic wave with these dipoles[5,6]. A mathematical model is then obtained which incorporates the physics and contains parameters that can be adjusted to fit the model to measured data. This approach is called parameter-based modeling and has the advantage that it also incorporates knowledge of the physical process into the model in addition to providing a fit to measured data. In particular, it incorporates the fact that the real and imaginary parts of ε_r are not independent of each other. In fact, a dielectric which exhibits loss will also exhibit dispersive behavior (real part of ε_r varies with frequency). A model based on the Debye equation[5] will be used, although it is not quite as rigorous as other models[4].

Although most soils are not classified as good conductors like the metals, most do support conduction currents. The conduction current leads to ohmic losses, and must be included in the model. The conduction is due to the presence of ionic salts in the soil, and tends to increase as the water content of the soil increases. Thus conduction will be a highly variable contribution to the losses in the soil. The conductivity is characterized by the static (zero frequency) conductivity, σ, and is easily measured by applying a static electric field $\mathbf{E}$ and measuring the current density $\mathbf{J}$

$$\mathbf{J} = \sigma \mathbf{E}. \tag{10}$$

When dealing with sinusoidal steady-state analysis, it is often convenient to combine the conduction currents and displacement currents since (in this case) they are both proportional to the electric field. This approach leads to a total complex relative dielectric constant

$$\varepsilon_r = \varepsilon_{r,dielectric} - j\frac{\sigma}{\omega \varepsilon_0}. \tag{11}$$

Using the Debye model[5],

$$\varepsilon_r' = \varepsilon_{r\infty}' + \sum_n \frac{\Delta \varepsilon_n'}{1 + \omega^2 \tau_n^2}, \tag{12}$$

and

$$\varepsilon_r'' = \frac{\sigma}{\omega \varepsilon_0} + \sum_n \frac{\Delta \varepsilon_n' \omega \tau_n}{1 + \omega^2 \tau_n^2}, \tag{13}$$

where τ_n is a relaxation time associated with the n^{th} nearby resonance and $\varepsilon'_{r\infty}$ is the essentially constant contribution due to the terms associated with the remaining higher, far away resonances. Using values of ε_r measured at different frequencies for a particular soil sample, the parameters $\varepsilon'_{r\infty}$, $\Delta\varepsilon'_n$, τ_n, and σ can be determined to provide a fit to the data. However, the fit is not unique since the number of terms in the summation is not specified. Nevertheless, this approach does guarantee that the real and imaginary parts of ε_r are coupled as the dipole theory suggests, and therefore contains information not available in a simple curve fit.

Several soils types were chosen as representative soils for this study. Fig. 1 shows the real and imaginary parts of the relative dielectric constant for four soil types. The gray San Antonio clay loam[7] represents an ionic soil which has significant conductivity. As the water content increases, it becomes very lossy. The sample with 20% water by weight represents a worst case, while the 5% water sample is probably more of a "typical" soil. The dry sand[6] represents a soil type which is more ideal for penetration by electromagnetic waves.

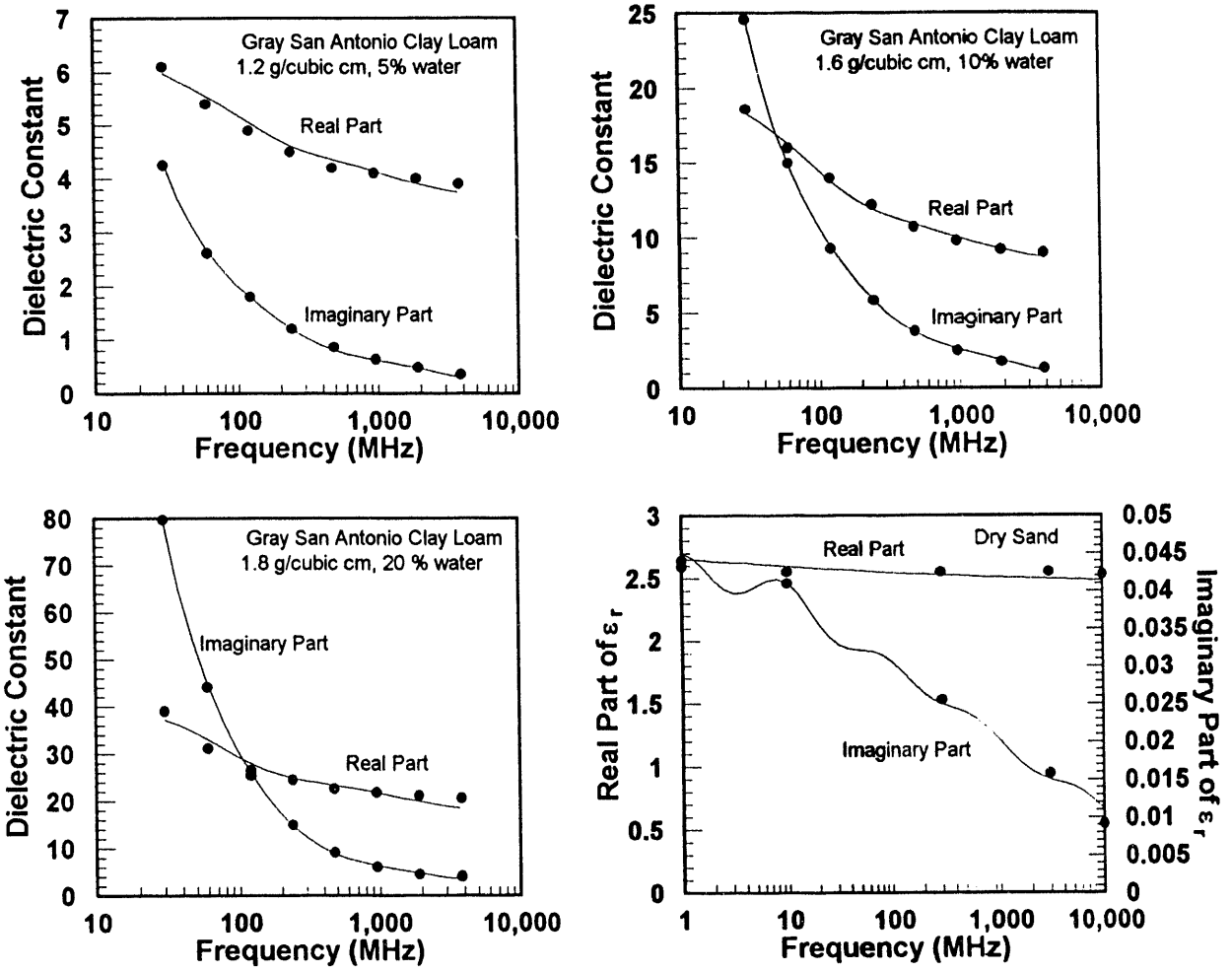

Fig. 1 Dielectric constant as a function of frequency for several representative soils: gray San Antonio clay loam with moisture contents of 5%, 10%, and 20% by weight[7], and dry sand[6]. The solid curves represent the parameter-based models used in the analysis, and the dots represent values obtained from the referenced literature.

3.2 Backscattering coefficient for rough soil

The scattering coefficient σ^0 (radar cross section per unit illuminated area) has been measured for various terrain types at various aspect angles and frequencies[8]. These data show that scattering depends on the complex dielectric constant, the angle of incidence, and the wavelength of the incident signal as well as parameters which describe the surface variations

(surface roughness). These data indicate that, as expected, the magnitude of the backscatter return is dependent on frequency and terrain type, but also the functional form, as a function of incident angle, changes with frequency and terrain type. Several scattering models have been developed which are applicable for different sets of conditions.

Three different models are used here, depending on the size of the roughness parameters measured in wavelengths. The models are[9] 1) the Kirchhoff scalar approximation, 2) the Kirchhoff stationary-phase approximation, and 3) the small perturbation model. Fig. 2 shows the regions of validity for each of these models, where the parameters are the surface-height standard deviation and the correlation length (both measured in wavelengths). Note that there are some regions in the $\sigma/\lambda - l/\lambda$ plane which are not covered by either of the three models. There are also regions where the Kirchhoff scalar approximation and the small-perturbation model are both valid. Unfortunately, when both models are valid, they do not agree precisely. In the estimates provided here, the small-perturbation model is used in preference to the Kirchhoff scalar approximation when both are valid. Details of the application of these models are reported elsewhere[4].

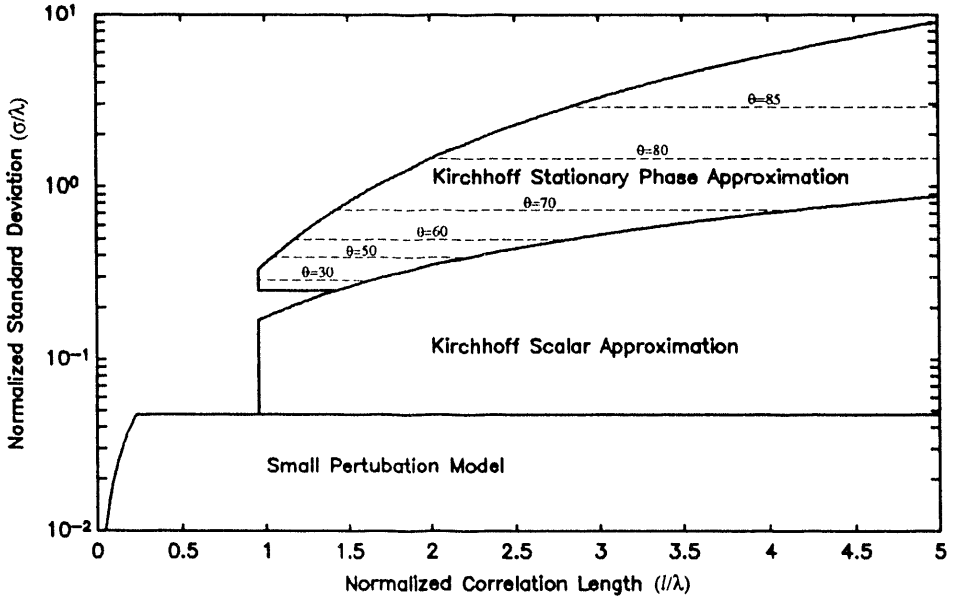

Fig. 2 Regions in the $\sigma/\lambda - l/\lambda$ plane which can be modeled by the three clutter models used in this study.

3.3 Clutter area

The clutter radar cross section is simply the pixel area A_{pixel} multiplied by the clutter backscatter coefficient σ^0. The slant range resolution of a synthetic-aperture radar is determined by the signal bandwidth. For an unweighted-chirp waveform, the slant-range resolution, Δr, is

$$\Delta r = \frac{c}{2\delta f}, \tag{14}$$

where f is the center frequency and δ is the fractional bandwidth of the signal. If we assume that the along-track or azimuth resolution is the same as the slant-range resolution, then the pixel area on the ground (the clutter area) is

$$A_{clutter} = A_{pixel} = \frac{\left(\frac{c}{2\delta f}\right)^2}{\cos\theta}. \tag{15}$$

The $\cos\theta$ in the denominator accounts for the lengthening of the across-track ground dimension as the incidence angle θ increases.

3.4 Target models

The targets will be modeled using spheres, cylinders, and flat plates. Rayleigh objects (objects with dimensions smaller than a wavelength) and resonant objects will be incorporated into the models of each of the three specific shapes. The models will be based on the free-space radar cross section, but the wavelength will be scaled according to the dielectric constant of the soil in which the object is buried. Thus, an object of a given size buried in soil will behave as if it were a larger but similar object in free space. This is not rigorous, but the approach is justified by the effort required to formulate the radar cross section rigorously for objects embedded in a lossy dielectric (which may be an appropriate task for an extended study).

The exact backscatter cross section for a conducting sphere with radius a is given by the well-known Mie series[10], while the cylinder model is based on the exact solution for the scattering width of an infinite-length cylinder[10]. The length of the cylinder is used to compute the total cross section, but the diffraction effects of the ends are ignored. The backscatter cross section of the flat plate is based on a low-frequency model valid when $ka < 1.25$ and a physical optics (high-frequency) model valid when $ka \geq 3.75$ with a mid-frequency curve fit which joins the two models[11].

4. SIGNAL-TO-CLUTTER ESTIMATES

4.1 Propagation loss in soil

The two-way propagation loss is plotted in Fig. 3 as a function of frequency for the four soil types. Although the magnitude of the imaginary part of the relative dielectric constant decreases as frequency increases (Fig. 1), the loss per meter increases because the wavelength decreases as frequency is increased, and loss (in dB) is proportional to the distance in wavelengths. Increased water content in the San Antonio clay loam dramatically increases the loss because of increased static conductivity.

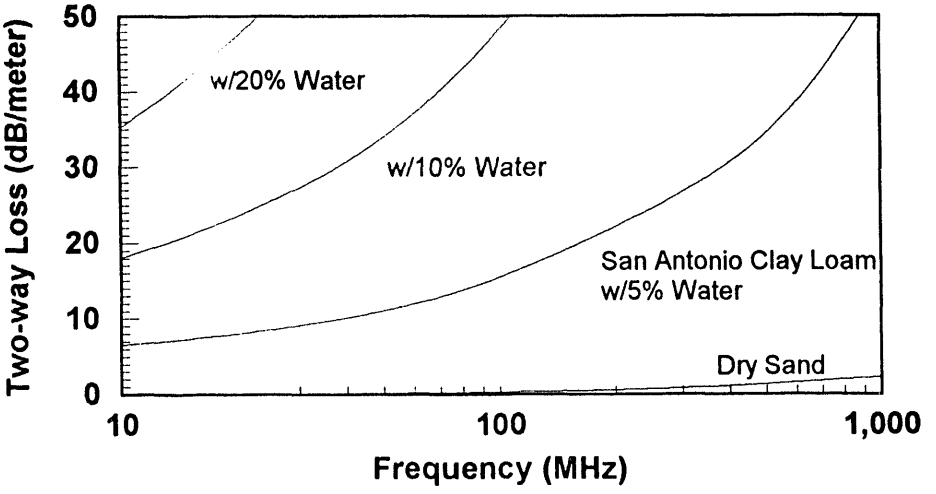

Fig. 3 Two-way propagation loss in dB/meter for a plane wave propagating in the soil models used in this study.

4.2 Two-way transmissivity at soil-air interface

The transmission from the air into the soil and from the soil back into the air at the air-soil interface, exclusive of all other losses, is termed the two-way transmissivity. The two-way transmissivity is the product of the incoming and outgoing transmission coefficients and is a function of the polarization, the soil type, and the angle of incidence. The angle of incidence is defined as the angle between the propagation direction and the surface-normal vector.

Fig. 4 shows the two-way transmissivity, based on plane-wave incidence, for the four soil types as a function of incident angle. The frequency is 100 MHz. Vertical polarization offers some advantage for large incident angles. Note the appearance of a damped Brewster effect near 80° incidence for San Antonio clay loam. The transmissivity is nearly constant or increases slightly as the incidence angle increases for vertical polarization, while it decreases monotonically for horizontal polarization. Since the dielectric properties of the soil are frequency dependent, the transmissivity is also frequency

dependent as illustrated in Fig. 5. Note that the transmissivity decreases as the frequency is decreased. Thus, although higher frequencies exhibit more severe propagation loss, they apparently couple across the soil-air interface more efficiently.

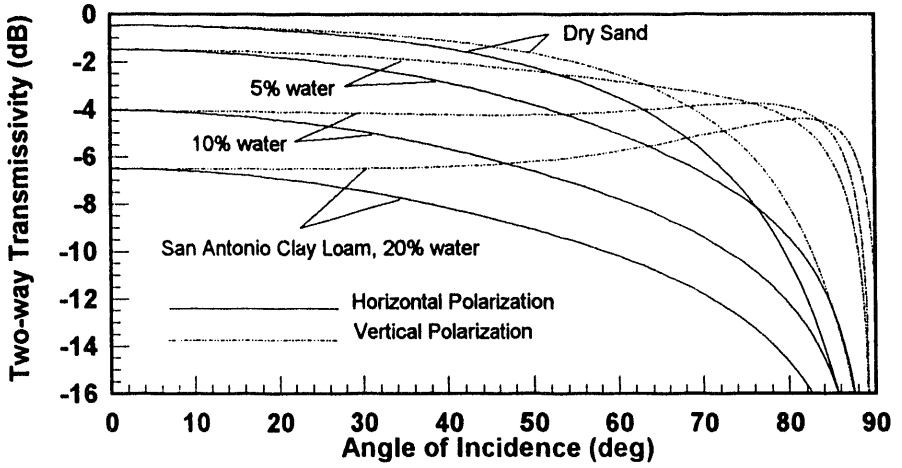

Fig. 4 Two-way transmissivity for the four soil types as a function of the incident angle for $f = 100$ MHz.

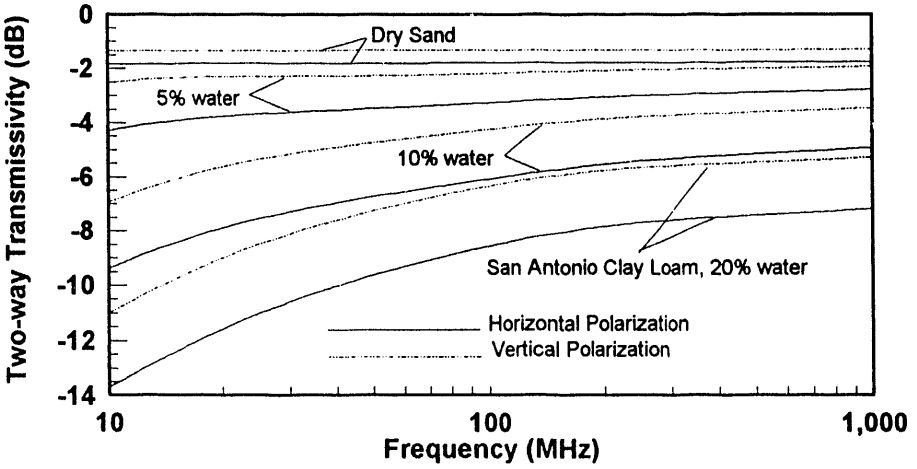

Fig. 5 Two-way transmissivity as a function of frequency for the four solid types at an angle of incidence of 45°.

4.3 Surface backscatter coefficient, σ^0

The backscatter from the random surface (clutter) depends on the soil dielectric constant and parameters describing the surface roughness. The surface-height standard deviation, σ_c, is specified along with a correlation length, L, which describes how quickly the surface roughness spectrum becomes uncorrelated with distance[9]. One of the three models described above is used, depending on the frequency, angle of incidence, σ_c, and L (see Fig. 2). Fig. 6 shows the variation in the backscatter coefficient as a function of incident angle at 100 MHz for a surface with small, rapid height variations ($\sigma_c = 7.5$ cm, and $L = 1$ m). Both vertical and horizontal polarizations are shown. As expected, clutter is reduced as the angle of incidence is increased. As the incident angle increases, vertical polarization exhibits the strongest backscatter (worst clutter) for this case. The small perturbation model was used for this calculation. Note that the model does not include the specular backscatter component at 0° incidence.

The frequency dependence of this same surface is described in Fig. 7 for an incident angle of 30°. Note that horizontal polarization has the greatest clutter return for frequencies below about 200 MHz where the small perturbation model is used, while vertical polarization is strongest for frequencies above 200 MHz, where the Kirchhoff model is used. This difference in the prediction of polarization behavior for the different models needs further study. The agreement between the small-

perturbation model and the Kirchhoff scalar approximation is fairly good for horizontal polarization, but the models differ by several dB for vertical polarization.

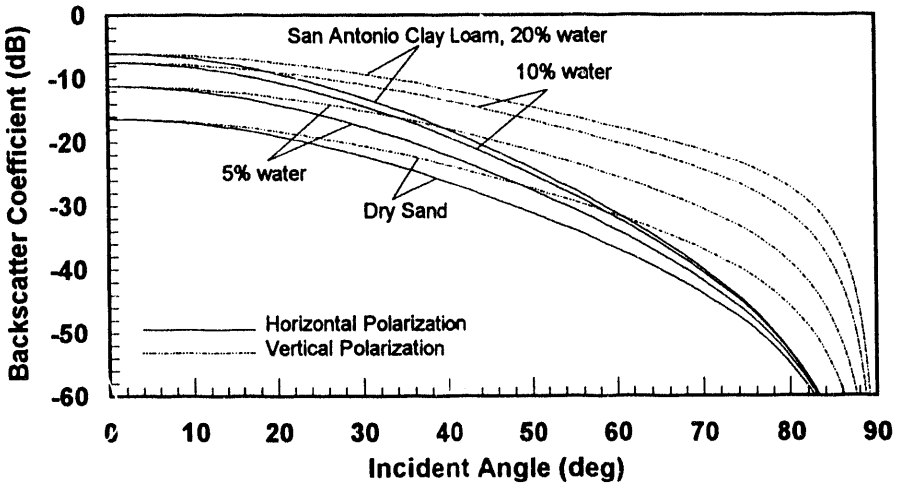

Fig. 6 Backscatter coefficient, σ^0, as a function of incident angle, θ, for four soil models with both horizontal and vertical polarization. The roughness standard deviation is $\sigma_c = 7.5$ cm, and the correlation length is $L = 1$ m. The frequency is 100 MHz.

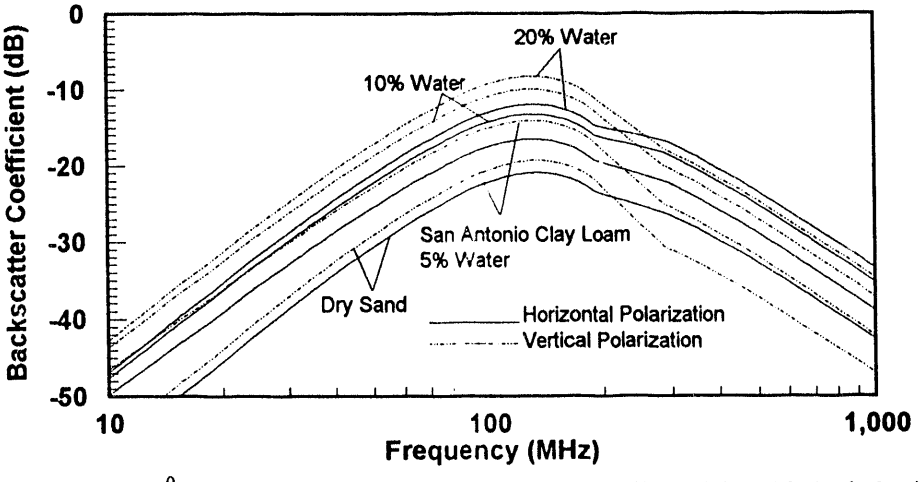

Fig. 7 Backscatter coefficient, σ^0, as a function of frequency for four soil models with both horizontal and vertical polarization. The roughness standard deviation , σ_c, is 7.5 cm and the correlation length, L, is 1 m. The incident angle is 30°.

4.4 Performance of canonical targets

The signal-to-clutter ratio for two small conducting spheres is illustrated in Fig. 8. The optimum frequency for both spheres is near 1 GHz. However, the larger sphere, buried in the dry sand, exhibits good signal-to-clutter performance down to at least 100 MHz, while the smaller sphere, buried in the San Antonio clay loam, shows good performance only above 300 MHz. The surface roughness for the dry sand is chosen to represent desert sand (σ_c= 0.5 m, L = 5 m), while the clay loam surface has smaller but more rapid variations (σ_c = 7.5 cm, L = 1 m).

A typical large buried pipe is modeled as a 0.5 m diameter cylinder 100 m long. Fig. 9 shows the predicted signal-to-clutter ratio when the pipe is buried 2 m below the surface of San Antonio clay loam with 5% water content, when viewed with an incidence angle of 30°, vertical polarization, and 50% bandwidth. Two surface-roughness conditions are illustrated: σ_c =

0.5 m, L = 5 m, and σ_c = 7.5 cm, L = 1 m. The surface with the larger standard deviation, σ_c, shows an optimum frequency near 200 MHz, while the shallower variation shows an optimum near 40 MHz. Thus, the condition of the surface (a parameter out of the control of the radar designer) is crucial in determining the optimum frequency for a SISAR.

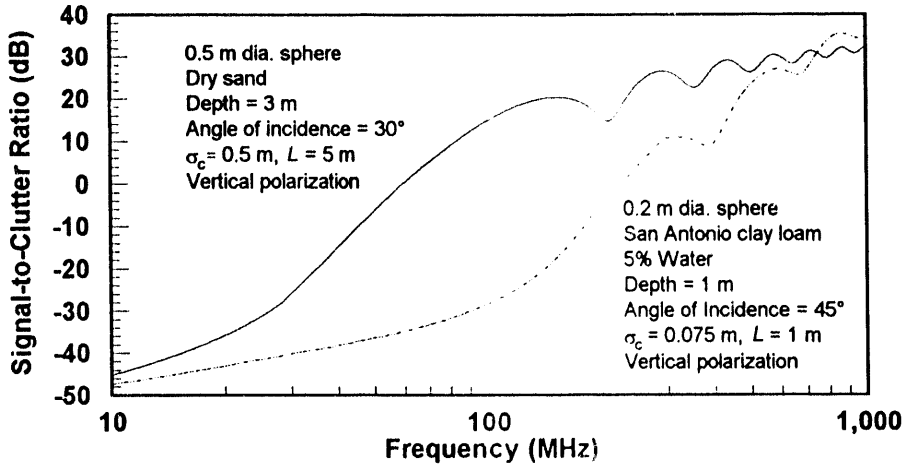

Fig. 8 Signal-to-clutter ratio for two spheres: a 0.5 m diameter sphere buried 3 m below the surface of dry sand, and a 0.2 m diameter sphere buried 1 m below the surface of San Antonio clay loam with 5% water content. The bandwidth is 50%.

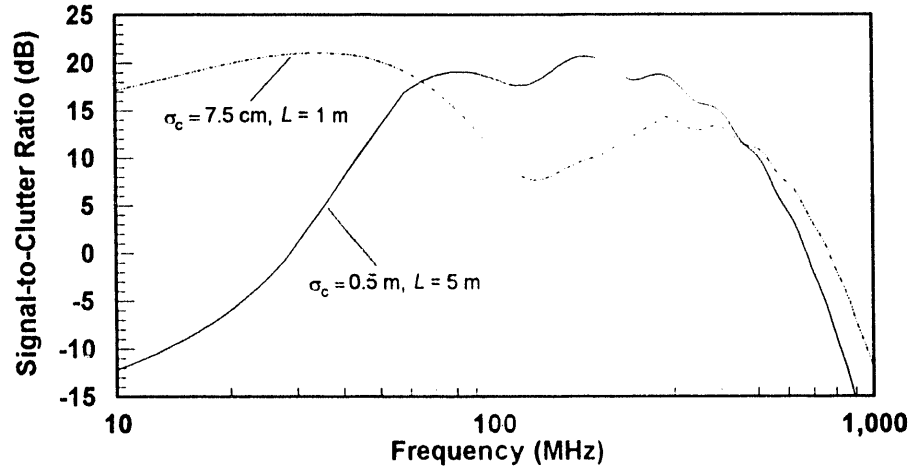

Fig. 9 Signal-to-clutter ratio for a 0.5 m diameter cylinder 100 m long buried 2 m in San Antonio clay loam with 5% water content. The curves correspond to two different surface-roughness conditions. The bandwidth is 50%, the angle of incidence is 30°, and the polarization is vertical.

The effect of varying the water content of the soil is seen in Fig. 10 which shows the signal-to-clutter ratio for a flat plate dihedral with a 30 m^2 area, buried 1 m below the surface. The polarization is vertical. Improved performance in the lossy soil is obtained through the use of high resolution (50% bandwidth) and a large incidence angle (45°). The clutter model in this example represents a gentle random surface. As the water content is increased, the optimum frequency (which is between 700 and 800 MHz for 5% water content) decreases, as does the maximum signal-to-clutter ratio. Performance is poor in the HF spectrum and best at UHF. Note that the dihedral is not detectable against the clutter when the water content reaches 20% by weight. Performance degrades rapidly as water is added to the soil, primarily because the static conductivity increases as a result of ionic salts going into solution.

5. CONCLUSIONS

The fact that a synthetic-aperture radar resolves a scene into small pixels improves the signal-to-clutter ratio of a SISAR over that obtainable with a conventional ground-penetrating radar. Even though the propagation loss in the soil increases with increasing frequency, the higher resolution obtainable with higher frequencies provides better signal-to-clutter performance at higher frequencies than is implied by the propagation-loss performance alone. For a specified target, burial depth, soil type, and signal bandwidth, an optimum frequency exists; neither using a higher nor a lower frequency will improve performance.

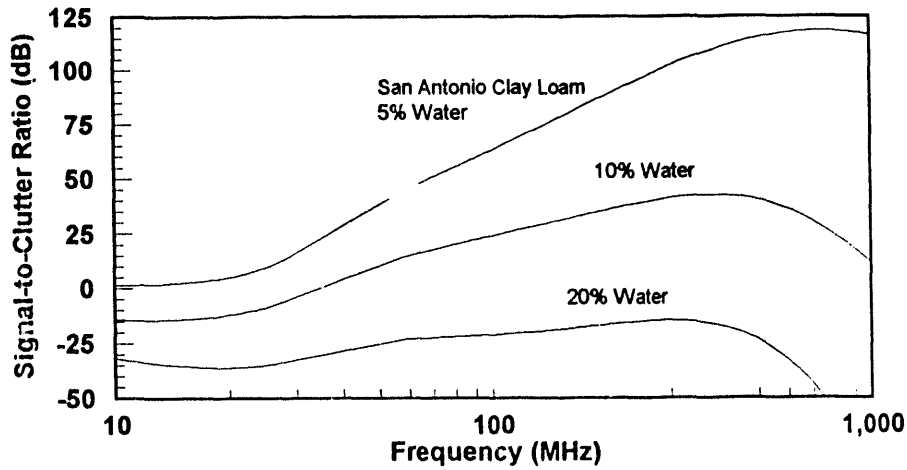

Fig. 10 Signal-to-clutter ratio for a 30 m^2 flat plate buried 1 meter in San Antonio clay loam with various percentages of water by weight. The signal bandwidth is 50 %, the angle of incidence is 45°, the polarization is vertical, the roughness standard deviation is 0.5 m, and the correlation length is 5 m.

For most of the situations examined in this study, the optimum frequency lies in the VHF and UHF portions of the spectrum, although some situations can be found where lower frequencies give better performance. For small angles of incidence, the lower frequencies (HF and low VHF) show better performance, but because the backscatter coefficient drops as the angle of incidence is increased, larger incidence angles (greater than about 40°) provide better performance at the upper VHF and UHF frequencies.

As predicted by the back-of-the envelope approach, the optimum frequency is higher for Rayleigh objects (small sphere, Fig. 8) than for flat-plate objects (Fig. 10) which have a higher optimum frequency than cylinders (Fig. 9). Also, as predicted, the optimum frequency decreases as the losses increase and as the object's burial depth is increased.

Unfortunately, one frequency is not optimum for all applications. A subsurface-imaging synthetic-aperture radar which has a tunable center frequency offers the potential to optimize its performance for a given mission. Such a radar could locate small (about a meter) conducting objects buried a few meters in dry sand by operating near 1 GHz or it could effectively locate long pipes buried about 1-2 meters in damp, ionic soil (which is very lossy) by operating near 100 MHz.

6. RECOMMENDATIONS

Additional study of surface-scattering models is warranted. The character of the surface roughness also needs to be studied in more detail to determine if multiple roughness scales are necessary to adequately describe the surface clutter. The current models do not cover all roughness scales of interest, and the agreement between the models in regions of overlapping validity is not adequate. Because the accurate description of the clutter is crucial to predicting SISAR performance, additional study in this area is warranted.

The current study ignores clutter due to volumetric scattering. A model for volumetric scattering needs to be developed and incorporated into the analysis. Volumetric clutter will compete with surface clutter to obscure buried targets.

The canonical target models used in this study are simple, conducting objects. The radar cross section is obtained from formulae for free-space scattering with the wavelength scaled to match the wavelength in the soil. Models are needed which predict the scattering from canonical objects embedded in a lossy half space, and which include dielectric objects, such as voids or caverns.

A limited number of soil types has been utilized in this study, and the types chosen may not be representative of soil types to be encountered in important applications of SISAR. Additional data exist in the literature for other soil types and for soils containing varying amounts of water. These data need to be incorporated into this study.

The effects of foliage on ground penetration have not been addressed. Additional study would be useful in determining the effect of grasses and other ground covers, since much of the earth's land area is covered by some type of plant life.

Soil is a dispersive media and the dispersion will distort the point-spread function of the synthetic-aperture radar and degrade the resolution obtainable for a particular signal bandwidth. Because the dispersion may be more severe in some portions of the spectrum than in others, it may have an effect on the choice of the optimum frequency through its effect on image resolution. This aspect of the dispersion has not been examined in this study, but it is important to do so in an expanded study.

7. ACKNOWLEDGMENTS

This work was performed at Sandia National Laboratories and supported by the U.S. Department of Energy under contract DE-AC04-76DP00789.

8. REFERENCES

1. A. W. Doerry, **A Model for Forming Airborne Synthetic Aperture Radar Images of Underground Targets**, Sandia National Laboratories Report SAND94-0139, January 1994.

2. M. I. Skolnik, ed., **Radar Handbook**, McGraw-Hill Book Co., New York, 1970. pp. 25-29 to 25-33.

3. G. G. Schaber, J. F. McCauley, C. S. Breed, G. R. Olhoeft, "Shuttle Imaging Radar: "Physical Controls on Signal Penetration and Subsurface Scattering in the Eastern Sahara", *IEEE Trans. Geoscience and Remote Sensing*, Vol. GR-24, No. 4, July 1986, pp 603-623.

4. B. C. Brock, W. E. Patitz, **Optimum Frequency for Subsurface-Imaging Synthetic-Aperture Radar**, Sandia National Laboratories Report SAND93-0815, May 1993.

5. C. A. Balanis, **Advanced Engineering Electromagnetics**, John Wiley & Sons, New York, 1989, Chapter 2.

6. A. R. Von Hippel, ed., **Dielectric Materials and Applications**, The Technology Press of M.I.T. and John Wiley & Sons, Inc., New York, 1954, pp. 21-24

7. J. E. Hipp, "Soil Electromagnetic Parameters as Functions of Frequency, Soil Density, and Soil Moisture", *Proceedings of the IEEE*, vol. 62, no. 1, January 1974, pp. 98-103.

8. F. T. Ulaby, M. C. Dobson, **Handbook of Radar Scattering Statistics for Terrain**, Artech House, Norwood, MA, 1989.

9. F. T. Ulaby, R. K. Moore, A. K. Fung, **Microwave Remote Sensing Active and Passive, Vol. II, Radar Remote Sensing and Surface Scattering and Emission Theory**, ch. 12, Addison-Wesley Publishing Co., Reading, Mass., 1982.

10. G. T. Ruck, D. E. Barrick, W. D. Stuart, C. K .Krichbaum, **Radar Cross Section Handbook, Volume 1**, Plenum Press, New York, 1970.

11. G. T. Ruck, D. E. Barrick, W. D. Stuart, C. K .Krichbaum, **Radar Cross Section Handbook, Volume 2**, Plenum Press, New York, 1970.

DATE
FILMED
5/4/94
END